Optical Fiber Technology 47 (2019) 152–157

Contents lists available at ScienceDirect

Optical Fiber Technology

journal homepage: www.elsevier.com/locate/yofte

All-fiber 2 μm thulium-doped mode-locked fiber laser based on $MoSe_2$-saturable absorber

Miaomiao Wu[a,b], Xing Li[a,b,*], Kan Wu[c,*], Duanduan Wu[a,b], Shixun Dai[a,b], Tiefeng Xu[a,b], Qiuhua Nie[a,b]

[a] Laboratory of Infrared Materials and Devices, The Research Institute of Advanced Technologies, Ningbo University, Ningbo 315211, China
[b] Key Laboratory of Photoelectric Materials and Devices of Zhejiang Province, Ningbo 315211, China
[c] State Key Laboratory of Advanced Optical Communication Systems and Networks, Department of Electronic Engineering, Shanghai Jiao Tong University, Shanghai 200240, China

ARTICLE INFO

Keywords:
All-fiber laser
$MoSe_2$-PVA
Passive mode-locking
Femtosecond pulse
Liquid-phase exfoliation

ABSTRACT

We demonstrate an all-fiber passive mode-locking laser operating in the 2 μm region that is implemented using a $MoSe_2$-based saturable absorber (SA). A $MoSe_2$-polyvinyl alcohol (PVA) SA is prepared with a modulation depth of 4.98%, a saturation intensity of 168.6 MW/cm^2 and a nonsaturable loss of 29.6%. When the $MoSe_2$-PVA SA was inserted into the fiber laser cavity, highly stable self-starting soliton pulse trains were generated with a center wavelength of 1943.35 nm and a 3 dB bandwidth of 4.38 nm. The pulse waveform has a $sech^2$ profile with pulse duration of 980 fs. The fundamental repetition rate is 23.53 MHz and the signal-to-background ratio of the fundamental frequency ranges up to 65 dB. The production of stable and robust pulses using this laser indicates that the $MoSe_2$-PVA SA is suitable for generation of 2 μm femtosecond ultrashort pulses.

1. Introduction

Because of advantages that include strong absorption of water or numerous chemicals and the presence of atmospheric transmission windows within their spectral range, all-fiber lasers in the 2 μm eye-safe region have been applied in a variety of fields, including laser spectroscopy [1], laser radar [2], free-space optical communications [3,4], and laser surgery. When the structure, size, cost and environmental stability of fiber lasers are taken into account, the use of saturable absorber-based mode-locking to generate ultrashort pulses in these lasers is regarded as a promising area for research. Therefore, it is very important to develop novel saturable absorber materials. However, for traditional saturable absorbers, such as dyes and semiconductor saturable absorber mirrors (SESAMs) [5,6], there are a number of unavoidable disadvantages and limitations, such as narrow operating bandwidths or requirements for expensive or complex fabrication processes, which have hindered the development of pulsed fiber lasers. When compared with the traditional materials, novel materials such as graphene oxide (GO) [7,8], graphite [9–12], carbon nanotubes (CNTs) [13–16], topological insulator (TI) [17], Black phosphorus (BP) [18], and transition metal dichalcogenides (TMDs) [19–21] can act as alternative nonlinear optical materials and allow new saturable absorbers to be developed. Among these saturable-absorber materials, TMDs have been regarded as the best potential materials from a technical viewpoint because of the layer-number-dependence of their band-gap properties [22]. TMDs are a class of materials with the general formula MX_2, where M is a transition metal (e.g., Mo, W, Nb), and X is a chalcogen (S, Se, Te). The TMD structure consists of quasi-2D layers that are weakly bound together by van der Waals forces [23]. There are more than 40 TMD materials, including WSe_2, $MoSe_2$, WS_2, WTe_2 and MoS_2. Recently, there have been many reports on all-fiber lasers that have used TMDs as saturable absorber materials [20,24,25]. Tang [26] and Stesmans [27] investigated the nonlinear saturable absorption properties of TMDs and found that the bandgap properties of these materials have a layer-number dependence, which offers huge potential with regard to various optoelectronic applications. Since then, there have been many studies of the saturable absorption properties of MoS_2 [27,28] and WS_2 [29,30] that were performed by applying these materials in Q-switched and mode-locked lasers operating in the wavelength regions of 1 μm and 1.5 μm [30–35]. However, when compared with sulfide-based TMDs, e.g., MoS_2 and WS_2, less technical attention has been paid to selenide-based TMDs such as $MoSe_2$ and WSe_2. To the best of the authors' knowledge, there have been few reports on the passive mode-locking of SAs based on selenide-based TMDs in the 2 μm wavelength region.

In this paper, we demonstrate the experimental realization of a

* Corresponding authors.
E-mail addresses: lixing1@nbu.edu.cn (X. Li), kanwu@sjtu.edu.cn (K. Wu).

https://doi.org/10.1016/j.yofte.2018.11.032
Received 5 August 2018; Received in revised form 8 November 2018; Accepted 26 November 2018
Available online 05 December 2018

thulium-doped fiber laser (TDFL) based on a $MoSe_2$-polyvinyl alcohol (PVA) SA at the 2 μm wavelength region. The $MoSe_2$-PVA structure is fabricated by the liquid-phase exfoliation method with a modulation depth of 4.98%, a saturation intensity of 168.6 MW/cm^2 and a non-saturable loss of 29.6%. When the $MoSe_2$-PVA SA film is inserted into the TDFL cavity, uniform pulse operation with a pulse duration of 980 fs is achieved at a fundamental repetition rate of 23.53 MHz. The center wavelength of the pulse is 1943.35 nm and the 3 dB bandwidth is 4.38 nm. The experimental results show that the $MoSe_2$-PVA SA is promising for use in femtosecond mode-locked fiber lasers operating in the 2 μm wavelength region.

2. Material preparation and characterization

The liquid-phase exfoliation method [29,36,37] was used to obtain a high-quality $MoSe_2$-PVA SA with a thin form for use in these experiments. Initially, $MoSe_2$ powder was dissolved in a sodium cholate (SC) solution with a ratio of 1.5 mg/ml. The SC was used as a surfactant and the suspension was sonicated in a laboratory ultrasonic cleaner with 100% power output for 1 h. No heating was required during crushing. The dispersions, which were collected in a special container, were then centrifuged at 5000 rpm for 90 min to remove any unaffiliated dispersions, and approximately 2/3 of the upper supernatant was collected using a pipette. The concentration of the $MoSe_2$ nanosheets within the solvent was approximately 0.015 mg/ml. A detailed illustration of the preparation of the $MoSe_2$ dispersions is shown in Fig. 1(a). Simultaneously, a 50 mg/ml polyvinyl alcohol (PVA) aqueous solution was also prepared. The $MoSe_2$/SC solution was then mixed with the 50 mg/mol PVA solution at a ratio of 1:5 for 36 h using a magnetic stirrer. Subsequently, the mixture was processed for another 6 h via an ultrasonic water bath device. Finally, we transferred the uniform $MoSe_2$ solution onto a quartz glass sheet and dried it at 50 °C for 5 days to produce a thin film with a thickness of 30–50 μm. To allow the experiment to proceed smoothly, the film was cut into a series of very small pieces (1 × 1 mm), as shown in Fig. 1(b); a few of these pieces were then sandwiched between the two FC/PC fiber ferrules using a fiber connector.

The power-dependent nonlinear transmission is well known to be the most important parameter for SA evaluation. The saturable absorption properties were investigated via a standard two-arm experiment using the setup shown in Fig. 2(a). The experiment setup consists of a home-made thulium-doped mode-locked fiber laser, a tunable optical attenuator, a 90:10 coupler, and two optical power meters. Femtosecond pulses were generated by a home-made mode-locked laser with a repetition rate of 50 MHz and a pulse width of 800 fs. The center wavelength was 1960 nm and the maximum output power was 25 mW. The power of the light that was transmitted through the sample was measured using power meter 2. A tunable optical attenuator was inserted after the mode-locked fiber laser to adapt the output to the measurement range of the power meter. Regulation of the output power of the mode-locked laser can be used to vary the transmission at different optical intensities, as clearly indicated by the results in Fig. 2(b). From the fitted curve, we conclude that the saturation intensity, the modulation depth and the nonsaturable loss are 168.6 MW/cm^2, 4.98%, and 29.6%, respectively.

3. Experimental setup and discussion

The experimental setup used for our thulium-doped mode-locked fiber laser based on the $MoSe_2$-PVA SA is shown in Fig. 3. The gain medium is a 0.25-m-long thulium-doped fiber (SM-TSF-5/125, Nufern) with high absorption of ∼340 dB/m at the pump laser wavelength of 1560 nm. The group velocity dispersion (GVD) of the gain fiber is −44.75 fs^2/mm. A 1560 nm pump laser (VFLS-1550-B, Connet-Laser Inc.) with a maximum power of 2 W is applied directionally to act as the pump source; the beam entered the gain medium through 1560/2000 nm wavelength division multiplexers (WDMs). Then, a 10/90 fiber coupler is used to extract 10% of the propagating light from the oscillator. The pigtails of the all-fiber devices were made from the single mode fiber SMF-28e$^+$, which has an estimated GVD of −71 fs^2/mm at 1950 nm. Subsequently, a 1 mm × 1 mm $MoSe_2$-PVA SA film is sandwiched between the two ferrules of an optical FC/PC connector. A polarization controller (PC) is used to adjust the polarization of the optical light and the birefringence of the fiber cavity. A polarization-insensitive optical isolator is inserted after the PC to ensure unidirectional light propagation. The length and the net dispersion of the resulting cavity were 8.5 m and −0.6 ps^2, respectively.

The evolution of the average output power versus the pump power is shown in Fig. 4(a). Fundamental mode-locking can be obtained easily when the pump power is raised to 500 mW and can be sustained stably at pump powers ranging from 456 mW to 660 mW. The maximum output power of the fundamental mode-locking fiber laser is 8.2 mW at a pump power of approximately 660 mW. The maximum output power of the fundamental mode-locking fiber laser can reach 9.3 mW at a pump power of approximately 660 mW by fine-tuning the PC. However, the laser mode locking is not very stable at this time, and it can only

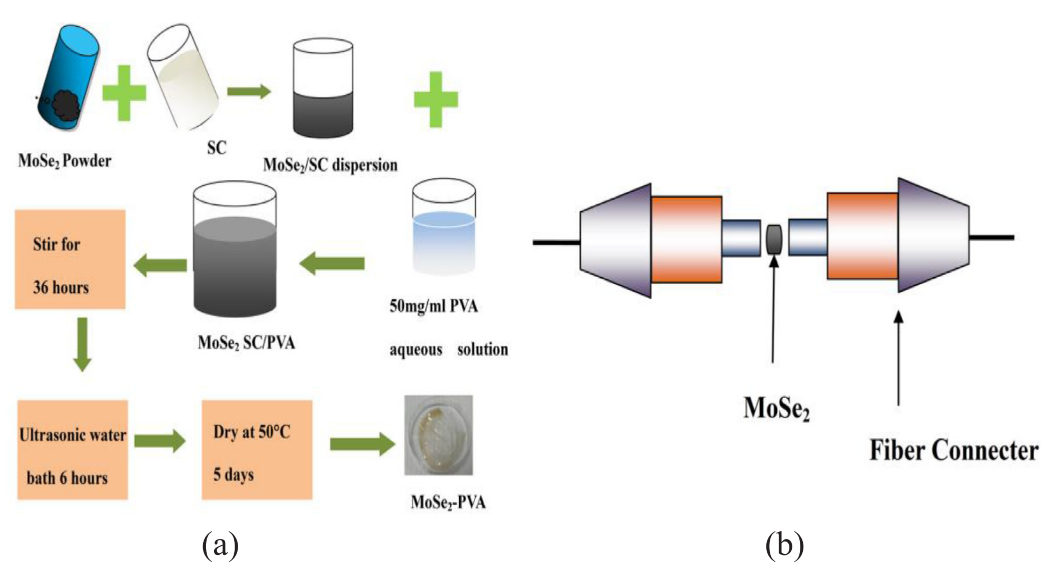

Fig. 1. (a) $MoSe_2$-PVA film fabrication procedure; (b) 1 mm × 1 mm $MoSe_2$-PVA SA film sandwiched between the two ferrules of an optical FC/PC connector.

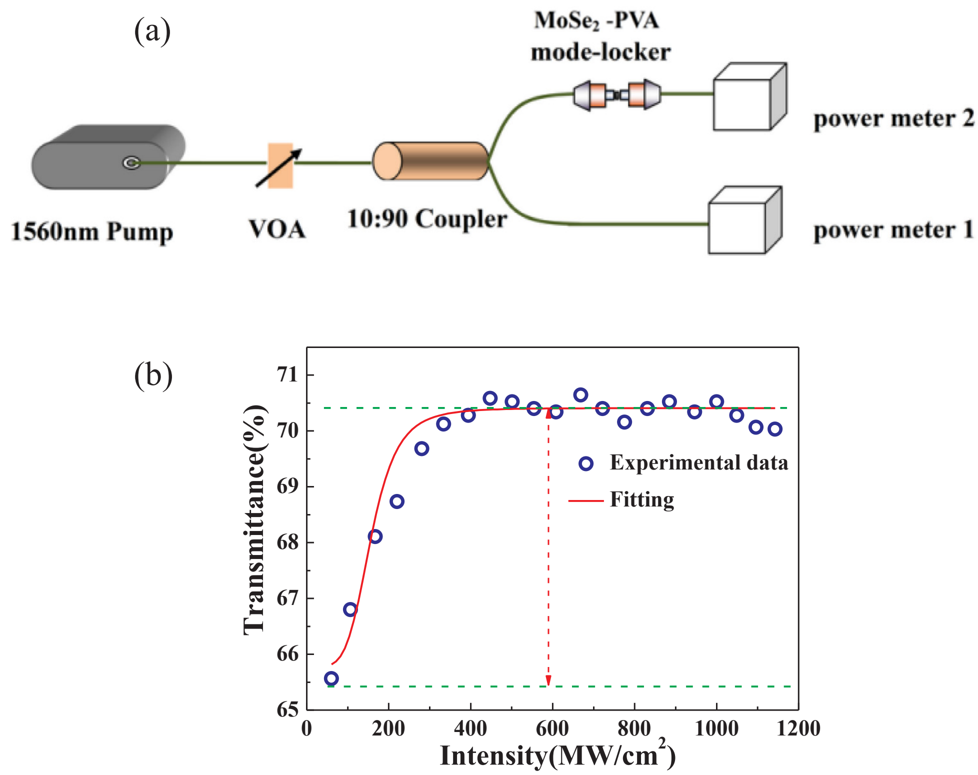

Fig. 2. (a) Experimental setup used for nonlinear transmission measurement of the $MoSe_2$-PVA SA. (b) Saturable absorption properties of the $MoSe_2$-PVA SA.

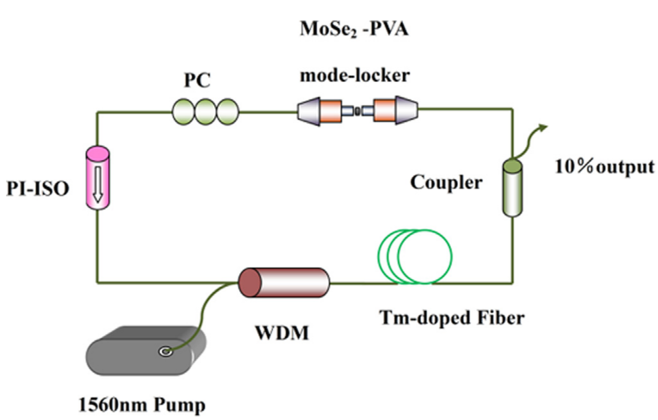

Fig. 3. Setup of the ring-cavity mode-locked fiber laser with the 1560 nm pump laser. WDM: wavelength division multiplexer; PC: polarization controller; PI-ISO: polarization-independent isolator.

maintain for ten minutes. Considering the fundamental repetition rate of 23.53 MHz, the maximum pulse energy of 0.39 nJ is deduced. As shown in Fig. 4(b), the center wavelength of the optical spectrum is 1943.35 nm with a 3 dB bandwidth of 4.38 nm at a pump power of 500 mW. The figure also shows that some Kelly sidebands are distributed asymmetrically on both sides of the spectrum; these sidebands were attributed to the periodic disturbances that occurred in the cavity during soliton mode-locking operations. Additionally, it should also be noted that some absorption peaks, marked using red spots, were scattered in the spectrum from 1940 nm to 1950 nm. These absorption peaks occur as a result of water absorption. It was also noted that the dip sideband that occurred at 1941.4 nm, which is indicated using a green spot, differs from the other dips around it. This dip was not attributed to four-wave-mixing, but was in fact caused by the slow saturable absorption properties of $MoSe_2$. In the experiment, we did not observe the phenomenon of dissipative soliton mode locking by adjusting the PC and pump power. But when the pump power was greater than 660mW, the multi-soliton operation can be observed in passively mode-locked soliton fiber lasers due to the peak limiting effect. However, we did not observe stable harmonic mode locking even if the PC and pump power are adjusted.

As shown in Fig. 5(a), the uniform pulse train in the time domain was detected using a 12 GHz photodetector (818-BB-51F, Newport) and analyzed using a 500 MHz oscilloscope (DLM2054, Yokogawa) to confirm the stability of the mode-locking operation. The pulse interval was 42.5 ns, corresponding to a fundamental repetition rate of 23.53 MHz. The autocorrelation trace in Fig. 5(b) shows that the fiber laser delivers a pulse train with a duration of 1.512 ps. Therefore, the pulse duration is 980 fs if we assume that the pulse waveform has a $sech^2$ profile. Mode locking was self-starting maintained for 24 h with negligible variations observed in the pulse parameters. The fluctuation of the laser's output power is less than 0.03 dB under over 8 h continuous monitoring. Note that it can self-start and work normally even laid in the laboratory environment after 30 days. The radio-frequency (RF) spectrum was also measured to evaluate the spectral quality of the mode-locking operation, with results as shown in Fig. 6. The extinction ratio is 65 dB within a 500 MHz span with a resolution bandwidth (RBW) of 1 kHz (N9000B Keysight). The signal noise is very high. I think there are two reasons for this result. Firstly, compared with other fiber lasers based on novel saturable absorber materials, our laser have higher output power of mode-locked pulses, which means it has greater signal power after a photodetector. Secondly, we use Agilent spectrum analyzer (N9000B) to measure the radio-frequency (RF) spectrum, which has a very low noise floor. In addition, in a 350 MHz span with an RBW of 10 kHz, no unwanted spurious sidebands were observed, thus indicating the high spectral purity of the mode-locking operation.

We also compared the output performance of the proposed mode-locked laser based on the TMD-based SA with those reported in previous investigations in the literature, with results as shown in Table 1. Four different SA-based mode-locked lasers appear to have similar output pulse characteristics. The saturation intensity of our $MoSe_2$ SA is

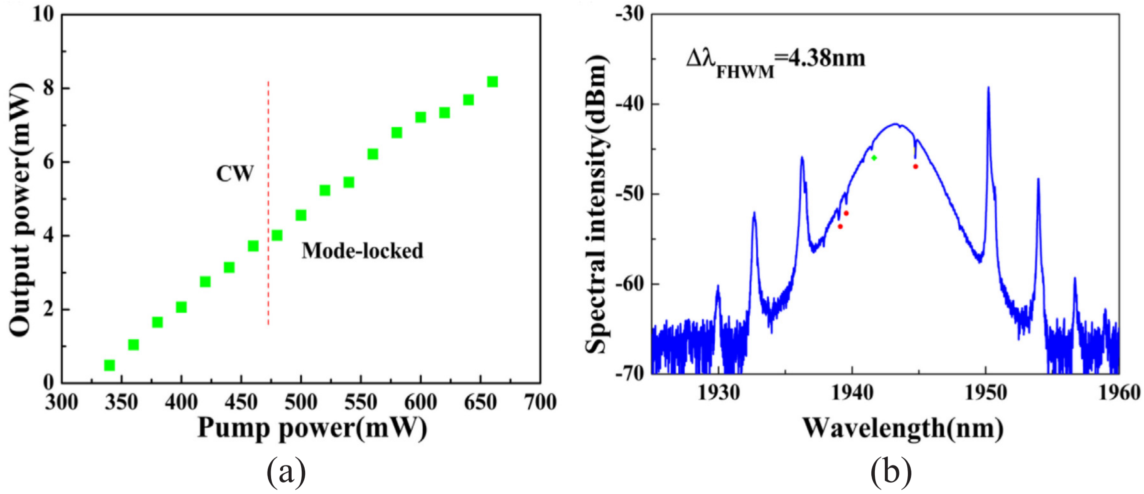

Fig. 4. (a) Output power versus pump power of the mode-locked laser based on the $MoSe_2$-PVA SA. (b) Optical spectrum.

much higher than those of the WS_2-based SA and the WSe_2 SA, whereas the pulse duration of our $MoSe_2$ SA is lower than the corresponding durations of the other TMD-based SAs. This is because WS_2-based SA has more attractive properties compared with other transition metal dichalcogenides (TMDs), including narrower bandgap between 1.1 eV (indirect) and 1.5 eV (direct), and larger spin-splitting energy of ~180 meV at the top of the valence bands. The narrow bandgap and larger spin-splitting energy could make $MoSe_2$ more applicable for ultrashort pulse generation. In addition, we can conclude from this comparison that $MoSe_2$ is a superior saturable-absorption material with the potential for application to femtosecond ultrashort pulse generation in the 2 µm wavelength range. We also compared the output performance of our $MoSe_2$ SA based mode-locked fiber laser with Black phosphorus (BP) SA based mid-infrared pulsed fiber laser at 3 µm wavelength, which is also shown in Table 1. Due to the larger unsaturated absorption loss, the pulse width of our mode-locked fiber laser is much smaller than that of mode-locked fiber laser based on BP SA.

4. Conclusions

In this work, we have demonstrated an ultrafast mode-locked fiber laser for operation in the 2 µm region that was implemented using a $MoSe_2$-based saturable absorber. The $MoSe_2$-PVA SA was prepared with a modulation depth of 4.98% and a saturation intensity of 168.6 MW/cm^2 for use in ultrashort pulse generation. Highly stable self-starting soliton pulse trains were generated using this SA at a repetition rate of 23.53 MHz. The fiber laser is centered at 1943.35 nm with a 3 dB bandwidth of 4.38 nm and delivers a pulse train with duration of 980 fs. High RF spectral purity with an extinction ratio of 65 dB was obtained during fundamental mode-locking. Our $MoSe_2$-based TDFL can be used as a seed source for 2 µm high-power pulsed fiber laser amplifiers and thus represents a considerable step towards the practical application of these lasers in areas such as special materials processing, medical diagnosis and mid-infrared super continuum generation. It is expectable to realize laser mode locking above 2 µm based on this $MoSe_2$-PVA saturable absorber, which is now under study. In addition, the number of layers of $MoSe_2$-PVA SA in a mode locked fiber laser would affect the cavity dynamics. Whether it is a key factor for the production of ultrashort pulses will be also investigated in our next step.

Acknowledgments

This work is partially supported by the Natural Science Foundation of Zhejiang Province, China (Grant Nos. LY19F050006), the National Natural Science Foundation of China (NSFC) (Grant Nos. 61627815, 61605096, 11804133 and 51567011), the Opened Fund of State Key Laboratory of Advanced Optical Communication Systems and Networks (Grant Nos. 2017GZKF16), the Open Fund of the Guangdong Engineering Technology Research and Development Center of Special Optical Fiber Materials and Devices (Grant Nos. 2016-3), and is

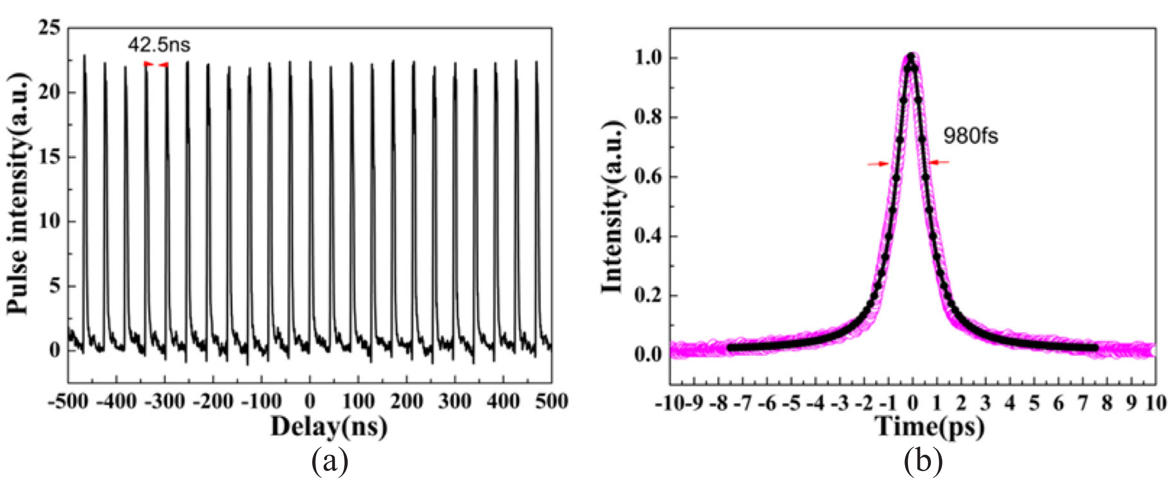

Fig. 5. (a) Oscilloscope trace, and (b) autocorrelation trace with circles indicating the measured data and solid line showing the sech^2 fit.

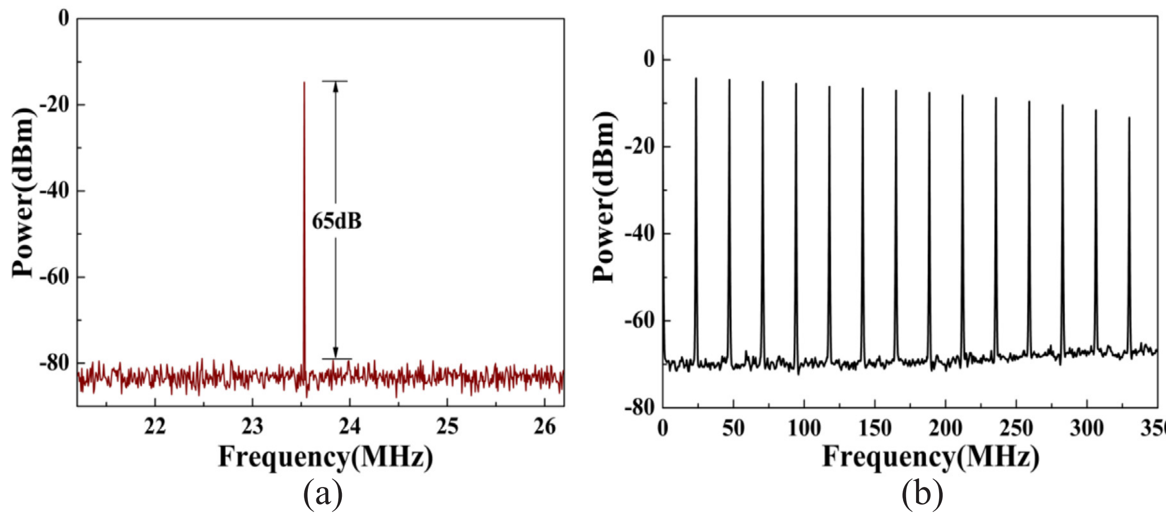

Fig. 6. (a) RF spectrum of the laser for a span of 500 MHz with a resolution bandwidth of 1 kHz and (b) a 350 MHz span with a resolution bandwidth of 10 kHz.

Table 1
Output performance comparison of our fiber laser with results from previous investigations of fundamental frequency mode-locked fiber lasers incorporating TMD-based SAs.

Saturable Absorption Material	MoS_2	WS_2	WSe_2	BP	$MoSe_2$
Saturation Intensity (MW/cm^2)	108.7	3.8	3.7	4.56	168.6
Nonsaturable Loss (%)	27.2	38.4	87	7.6	29.6
Modulation depth (%)	12.5	10.9	1.83	41.2	4.98
Pulse Wavelength (nm)	1927	1925	1863.96	2866.7	1943.35
Repetition rate (MHz)	13.9	34.8	11.36	13.987	23.53
Spectral Bandwidth (nm)	2.86	5.6	3.19	4.35	4.38
Pulse Width (ps)	1.51	1.3	1.16	8.6	0.98
Reference	[38]	[25]	[39]	[40]	This work

sponsored by the K. C. Wong Magna Fund in Ningbo University.

References

[1] F.J. McAleavey, J. O'Gorman, J.F. Donegan, B.D. MacCraith, J. Hegarty, G. Maze, Narrow linewidth, tunable Tm^{3+}-doped fluoride fiber laser for optical-based hydrocarbon gas sensing, IEEE J. Sel. Top. Quantum Electron. 3 (1997) 1103–1111.
[2] W. Ni-Meister, W. Yang, S. Lee, A.H. Strahler, F. Zhao, Validating modeled lidar waveforms in forest canopies with airborne laser scanning data, Remote Sens. Environ. 204 (2018) 229–243.
[3] J. Bohata, S. Zvanovec, M. Komanec, J. Jaros, Z. Ghassemlooy, Adaptation of transmitting signals over joint aged optical fiber and free space optical network under harsh environments, Optik 151 (2017) 7–17.
[4] K. Anbarasi, C. Hemanth, R.G. Sangeetha, A review on channel models in free space optical communication systems, Opt. Laser Technol. 97 (2017) 161–171.
[5] U. Parali, X. Sheng, A. Minassian, G. Tawy, J. Sathian, G.M. Thomas, M.J. Damzen, Diode-pumped Alexandrite laser with passive SESAM Q-switching and wavelength tunability, Opt. Commun. 410 (2018) 970–976.
[6] O.G. Okhotnikov, A.B. Grudinin, M. Pessa, Ultra-fast fibre laser systems based on SESAM technology: new horizons and applications, New J. Phys. 6 (2004) 177-177.
[7] J. Chang, H. Li, Z. Yang, N. Yan, Efficient and compact Q-switched green laser using graphene oxide as saturable absorber, Opt. Laser Technol. 98 (2018) 134–138.
[8] J. Zhao, Y. Wang, P. Yan, S. Ruan, Y. Tsang, G. Zhang, H. Li, An Ytterbium-doped fiber laser with dark and Q-switched pulse generation using graphene-oxide as saturable absorber, Opt. Commun. 312 (2014) 227–232.
[9] K.Y. Lau, F.D. Muhammad, A.A. Latif, M.H. Abu Bakar, Z. Yusoff, M.A. Mahdi, Passively mode-locked soliton femtosecond pulses employing graphene saturable absorber, Opt. Laser Technol. 94 (2017) 221–227.
[10] Q. Wang, T. Chen, B. Zhang, M. Li, Y. Lu, K.P. Chen, All-fiber passively mode-locked thulium-doped fiber ring laser using optically deposited graphene saturable absorbers, Appl. Phys. Lett. 102 (2013) 131117.
[11] J. Sotor, G. Sobon, K. Krzempek, K.M. Abramski, Fundamental and harmonic mode-locking in erbium-doped fiber laser based on graphene saturable absorber, Opt. Commun. 285 (2012) 3174–3178.
[12] Z.T. Wang, Y. Chen, C.J. Zhao, H. Zhang, S.C. Wen, Switchable dual-wavelength synchronously Q-switched erbium-doped fiber laser based on graphene saturable absorber, IEEE Photonics J. 4 (2012) 869–876.
[13] M.A. Solodyankin, E. Obraztsova, A. Lobach, A.I. Chernov, A. Tausenev, V.I. Konov, E. Dianov, Mode-locked 1.93 microm thulium fiber laser with a carbon nanotube absorber, 2008.
[14] M. Jung, J. Koo, Y.M. Chang, P. Debnath, Y.W. Song, J.H. Lee, An all fiberized, 1.89-μm Q-switched laser employing carbon nanotube evanescent field interaction, Laser Phys. Lett. 9 (2012) 669–673.
[15] M.A. Chernysheva, A.A. Krylov, P.G. Kryukov, E.M. Dianov, Nonlinear amplifying loop-mirror-based mode-locked thulium-doped fiber laser, IEEE Photonics Technol. Lett. 24 (2012) 1254–1256.
[16] A. Martinez, S. Yamashita, Multi-gigahertz repetition rate passively mode locked fiber lasers using carbon nanotubes, Opt. Express 19 (2011) 6155–6163.
[17] Y. Chen, C. Zhao, S. Chen, J. Du, P.H. Tang, G. Jiang, H. Zhang, S. Wen, D. Tang, Large energy, wavelength widely tunable, topological insulator Q-switched erbium-doped fiber laser, IEEE J. Sel. Top. Quantum Electron. 20 (2014) 315–322.
[18] J. Ma, S. Lu, Z. Guo, X. Xu, H. Zhang, D. Tang, D. Fan, Few-layer black phosphorus based saturable absorber mirror for pulsed solid-state lasers, Opt. Express 23 (2015) 22643–22648.
[19] K. Wu, X.Y. Zhang, J. Wang, X. Li, J.P. Chen, WS_2 as a saturable absorber for ultrafast photonic applications of mode-locked and Q-switched lasers, Opt. Express 23 (2015) 11453–11461.
[20] J. Lee, J. Koo, J. Lee, Y.M. Jhon, J.H. Lee, All-fiberized, femtosecond laser at 1912 nm using a bulk-like $MoSe_2$ saturable absorber, Optical Mater. Express 7 (2017) 2968.
[21] Z. Luo, D. Wu, B. Xu, H. Xu, Z. Cai, J. Peng, J. Weng, S. Xu, C. Zhu, F. Wang, Z. Sun, H. Zhang, Two-dimensional material-based saturable absorbers: towards compact visible-wavelength all-fiber pulsed lasers, Nanoscale 8 (2016) 1066–1072.
[22] W. Choi, N. Choudhary, G.H. Han, J. Park, D. Akinwande, Y.H. Lee, Recent development of two-dimensional transition metal dichalcogenides and their applications, Mater. Today 20 (2017) 116–130.
[23] S. Manzeli, D. Ovchinnikov, D. Pasquier, O.V. Yazyev, A. Kis, 2D transition metal dichalcogenides, Nat. Rev. Mater. 2 (2017) 17033.
[24] B. Chen, X. Zhang, K. Wu, H. Wang, J. Wang, J. Chen, Q-switched fiber laser based on transition metal dichalcogenides MoS_2, $MoSe_2$, WS_2, and WSe_2, Opt. Express 23 (2015) 26723–26737.
[25] M. Jung, J. Lee, J. Park, J. Koo, Y.M. Jhon, J.H. Lee, Mode-locked, 1.94-mum, all-fiberized laser using WS_2 based evanescent field interaction, Opt. Express 23 (2015) 19996–20006.
[26] Y. Ding, Y. Wang, J. Ni, L. Shi, S. Shi, W. Tang, First principles study of structural, vibrational and electronic properties of graphene-like MX_2 (M = Mo, Nb, W, Ta; X = S, Se, Te) monolayers, Phys. B: Condensed Matter 406 (2011) 2254–2260.
[27] E. Scalise, M. Houssa, G. Pourtois, V.V. Afanas′ev, A. Stesmans, First-principles study of strained 2D MoS_2, Phys. E: Low-dimensional Systems Nanostruct. 56 (2014) 416–421.
[28] Q. Yue, J. Kang, Z. Shao, X. Zhang, S. Chang, G. Wang, S. Qin, J. Li, Mechanical and electronic properties of monolayer MoS_2 under elastic strain, Phys. Lett. A 376 (2012) 1166–1170.
[29] B. Guo, Y. Yao, P.G. Yan, K. Xu, J.J. Liu, S.G. Wang, Y. Li, Dual-wavelength soliton mode-locked fiber laser with a WS_2-based fiber taper, IEEE Photonics Technol. Lett. 28 (2016) 323–326.
[30] K. Wu, X. Zhang, J. Wang, X. Li, J. Chen, WS_2 as a saturable absorber for ultrafast photonic applications of mode-locked and Q-switched lasers, Opt. Express 23 (2015) 11453–11461.
[31] L. Li, Y. Wang, X. Wang, G. Yang, S. Jiang, Z. Li, B. Man, Y. Wang, Er-doped mode-locked fiber laser with WS_2/fluorine mica (FM) saturable absorber, Opt. Laser Technol. 90 (2017) 109–112.
[32] L. Li, Y. Wang, Z.F. Wang, X. Wang, G. Yang, High energy Er-doped Q-switched fiber laser with WS_2 saturable absorber, Opt. Commun. 406 (2018) 80–84.
[33] X. Wang, J. Xu, Z. You, Y. Sun, Z. Zhu, C. Tu, Tri-wavelength passively Q-switched Yb^{3+}:$GdAl_3(BO_3)_4$ solid-state laser based on WS_2 saturable absorber, Opt. Mater. 62

(2016) 621–625.

[34] B. Chen, X. Zhang, C. Guo, K. Wu, J. Chen, J. Wang, Tungsten diselenide Q-switched erbium-doped fiber laser, Opt. Eng. 55 (2016) 081306.

[35] M. Zhang, R.C.T. Howe, R.I. Woodward, E.J.R. Kelleher, F. Torrisi, G. Hu, S.V. Popov, J.R. Taylor, T. Hasan, Solution processed MoS_2-PVA composite for sub-bandgap mode-locking of a wideband tunable ultrafast Er:fiber laser, Nano Res. 8 (2015) 1522–1534.

[36] S. Tongay, J. Zhou, C. Ataca, K. Lo, T.S. Matthews, J. Li, J.C. Grossman, J. Wu, Thermally driven crossover from indirect toward direct bandgap in 2D semiconductors: $MoSe_2$ versus MoS_2, Nano Lett. 12 (2012) 5576–5580.

[37] M. Chhowalla, H.S. Shin, G. Eda, L.J. Li, K.P. Loh, H. Zhang, The chemistry of two-dimensional layered transition metal dichalcogenide nanosheets, Nat. Chem. 5 (2013) 263.

[38] L. Cao, X. Li, R. Zhang, D. Wu, S. Dai, J. Peng, J. Weng, Q. Nie, Tm-doped fiber laser mode-locking with MoS_2 -polyvinyl alcohol saturable absorber, Opt. Fiber Technol. 41 (2018) 187–192.

[39] J. Wang, W. Lu, J. Li, H. Chen, Z. Jiang, J. Wang, W. Zhang, M. Zhang, I.L. Li, Z. Xu, W. Liu, P. Yan, Ultrafast thulium-doped fiber laser mode locked by monolayer WSe_2, IEEE J. Sel. Top. Quantum Electron. 24 (2018) 1–6.

[40] J. Li, H. Luo, B. Zhai, R. Lu, Z. Guo, H. Zhang, Y. Liu, Black phosphorus: a two-dimension saturable absorption material for mid-infrared Q-switched and mode-locked fiber lasers, Sci. Rep. 6 (2016) 30361.